Bulletin of the Seismological Society of America, Vol. 102, No. 5, pp. 2252–2256, October 2012, doi: 10.1785/0120110253

Short Note

Probability for Simulating Future Earthquakes with $M_w \geq 6.0$ in Taiwan for Seismic Hazard for the Earthquake Catalog from 1900 to 2008

by Kuei-Pao Chen, Yi-Ben Tsai, Wen-Yen Chang, and Chin-Tung Cheng

Abstract In this study, we use extreme value theory based on Gumbel-equation derivations to estimate the Gutenberg–Richter a and b parameters for Taiwan. Data are from the augmented, homogenized (in terms of moment magnitude), historic catalog for Taiwan. The island is divided into grids of 0.2° latitude by 0.2° longitude, and Gumbel type 1 statistical analysis is applied. The values of a and b are then used to determine the probability of large earthquakes ($M_w \geq 6.0$) occurring at each grid. The results show two relatively high probability paths for large earthquakes, one extending from Hsinchu southward to Taichung, Chiayi, and Tainan in western Taiwan and the other from Ilan southward to Hualian and Taitung in eastern Taiwan, both of which are characterized by low b-values. It indicates that future earthquakes can be expected along these paths characterized by low b-values. Additionally, maximum peak ground acceleration and maximum peak ground velocity (determined from respective attenuation laws and a gridding regimen of 0.1° latitude by 0.1° longitude for Taiwan) follow similar paths to that of the low b-values.

Introduction

The relation introduced by Gutenberg and Richter (1944) gives us the parameters a and b, which characterize a region's temporal and quantitative seismicity. Estimation of the two parameters can be derived from a number of statistical processes. For situations in which a complete catalog of earthquakes is not available, methods based on the statistics of extreme events (extreme value theory), using reduced variate probability plotting, have been applied (Turnbull and Weatherley, 2006). In the case of regional seismicity, the dataset of observations is invariably only a small subset of the region's seismic history. Additionally, if we use a dataset that does not contain enough data to sample adequately a full range of observable values, the estimated a- and b-values may contain significant errors. However, by applying extreme value theory, it is still possible to accurately estimate a- and b-values even when the sample data is extracted from source distributions.

The Fisher and Tippett (1928) probability distributions were specifically formulated to model extreme data values. They were able to prove that, depending on the distribution parameters used [$\xi, \theta(>0)$, and k (>0)], the generalized cumulative distribution of extreme value theory could be reduced to one of their three Fisher–Tippett distributions. These were previously summarized in Johnson *et al.* (1995).

Fisher–Tippett Type 1:

$$P_r[X \leq x] = \exp\{-\exp[-1/\theta(x-\xi)]\}. \quad (1)$$

Fisher–Tippett Type 2:

$$P_r[X \leq X] = 0, \quad \text{where } x < \xi,$$
$$= \exp\{-\exp\{-(1/\theta(x-\xi))k\}\}, \quad \text{where } x \geq \xi. \quad (2)$$

Fisher–Tippett Type 3:

$$P_r[X \leq x] = \{-\exp\{-(1/\theta(\xi-x))k\}\}, \quad \text{where } x \leq \xi,$$
$$= 1, \quad \text{where } x > \xi. \quad (3)$$

In equations (1–3), ξ is the shape parameter governing the tail behavior of the distribution, θ represents parameters either known or undetermined, and k is the cumulant parameter.

Sometimes the extreme value method is criticized for ignoring small value data; however, this criticism is not valid. The extreme value method is designed to specifically model the extreme value data of a distribution; inclusion of small value data would invalidate the method (Turnbull and Weatherley, 2006). Because in earthquake research the record of

large events (extreme value events) is generally well known, this aspect of the source data can be considered complete when estimating the parameters of the extreme value distribution, and therefore finite sampling issues are not a concern. Thus, in this study we used prescribed a and b parameters estimated from the extreme value theory to simulate the seismic activity for Taiwan.

Taiwan is located in the western Pacific at the collision zone between the Eurasian and Philippine Sea plates. The collision zone is complex with a change in subduction polarity between the north and south of the island. In northern Taiwan, the Philippine Sea plate northwardly subducts under the Eurasian plate, while in the southwestern offshore region the South China Sea lithosphere eastwardly subducts under the Luzon arc. The complexity of motion among the plates results in frequent earthquakes on and around Taiwan. The first seismograph on Taiwan was installed in 1897. This has given Taiwan a relatively complete earthquake catalog since that time. The catalog has been augmented and homogenized to reflect moment magnitude across Taiwan by Chen and Tsai (2008) and Chen *et al.* (2010). Figure 1 is from Chen *et al.* (2010). It shows the complete dataset for earthquakes of magnitude $M_w \geq 5.0$. From Figure 1, we can see that earthquakes occur very frequently around Taiwan, especially along the eastern margins. This frequent seismic activity along the east coast provides ample seismic data.

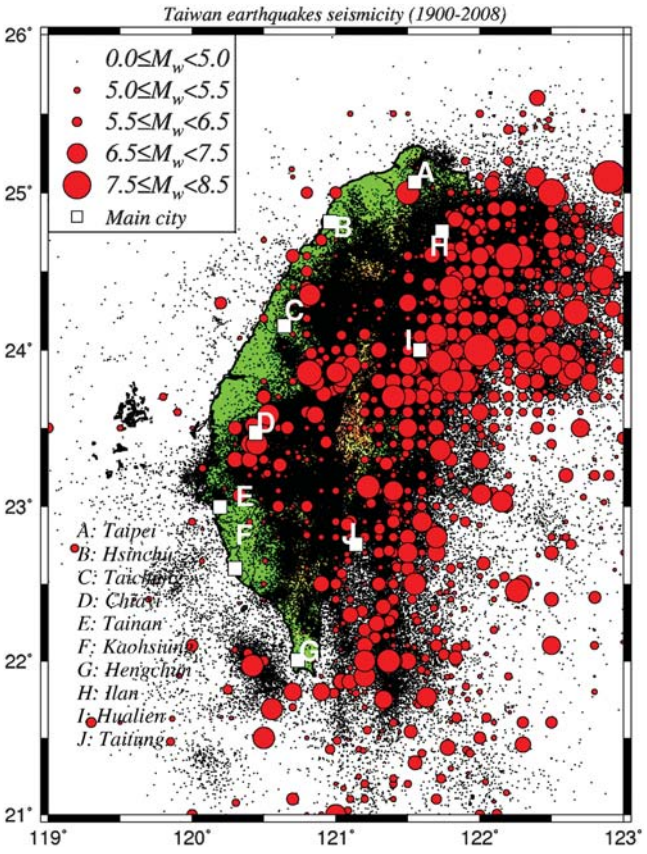

Figure 1. Seismic activity of Taiwan from 1900 to 2008.

Alternatively, earthquakes occur less often in western Taiwan but can be of great intensity. Much of Taiwan's industry and population exist in these western regions, and therefore accurate estimation of the probability of large earthquake occurrence is very important. In this study, we divide Taiwan into small elements of grids (0.2° latitude by 0.2° longitude) and estimate the probability of a future earthquake of $M_w \geq 6.0$ (large earthquake) occurring for each of the elements. On a relative probability basis, for western Taiwan, we find that the high probability path for a large earthquake extends southward from Hsinchu to Taichung, Chiayi, Tainan, and Kaohsiung; for eastern Taiwan, the high probability path is from Ilan southward to Hualian and Taitung. These paths are shown to have low b-values, which indicate future earthquakes. Additionally, the paths described in this study show high peak ground acceleration (PGA), which means coseismic destructive shaking can be expected. These results should be of interest to city planners and construction engineers.

Using the Gumbel Distribution to Estimate a and b Parameters

The Gumbel distribution is a particular case of the Fisher–Tippett distribution and is used in this section to estimate the Gutenberg–Richter a and b parameters. Lomnitz (1974) showed that a homogeneous earthquake process with cumulative magnitude distribution can be expressed as

$$F(m;\beta) = 1 - e^{-\beta m}, \qquad m \geq 0. \tag{4}$$

According to the Gumbel (1958) cumulative distribution function, the maximum annual earthquake magnitude can be expressed as

$$G(y;\alpha,\beta) = \exp[-\alpha \exp(-\beta y)], \qquad y \geq 0, \tag{5}$$

where α is the average number of earthquakes with magnitude > 0.0 per year, β is the inverse of the average magnitude of earthquakes under the considered region, and y is the maximum annual earthquake magnitude. Using the probability integral transformation theorem, and manipulating equation (5), we obtain the following relation:

$$-\ln[-\ln(p_m)] = \beta y_i - \ln(\alpha), \tag{6}$$

where p_m represents the plotting position. Gumbel (1958) proposed two models: one is $p_m = \frac{m}{n+1}$, which calculates the mean frequency of the m-th observation, and the other is a more sophisticated model $p_m = \frac{m-0.3}{n+0.4}$, where n is total observed data, and the $-\ln[-\ln(p_m)]$ is the reduced variate. Comparison of the difference between the two models is shown in Figure 2. From Figure 2a,b, we can see they are almost the same. The relationship between Gumbel parameters α and β and Gutenberg–Richter parameters a and b can be expressed as

$$b = \beta \log_{10} e, \tag{7}$$

and

$$a = \log_{10} \alpha. \tag{8}$$

From Figure 2a,b, because the a- and b-values calculated from the two models are almost the same, we adopt the simpler model $p_m = \frac{m}{n+1}$.

Simulating Future Earthquakes

The Gutenberg and Richter (1944) seismicity relation of earthquake frequency versus magnitude can be expressed as

$$\log_{10} N = a - bM, \tag{9}$$

where N is the number of earthquakes with magnitude $\geq M$, and a, b are constants. We can rewrite the equation (9) as

$$N = 10^{a-bM}. \tag{10}$$

If the occurrence of an earthquake is a random process (Poisson process), then the probability of at least one earthquake occurring of magnitude $\geq M$ within one year is

$$p = 1 - e^{-N} = 1 - e^{-10^{a-bm}} = 1 - e^{-e^{\ln 10^{a-bm}}}. \tag{11}$$

After derivation, we obtain the relation

$$M = \frac{a}{b} - \frac{1}{b \ln 10} \ln[-\ln(1-p)], \tag{12}$$

where p is a random number for the interval (0,1).

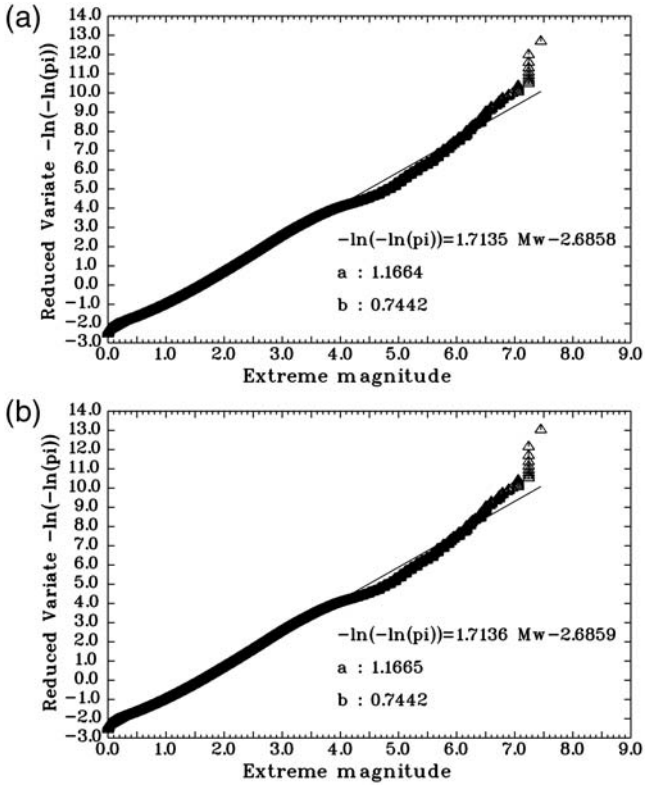

Figure 2. Demonstration of Gumbel probability plots for Taiwan using (a) position [$p_m = \frac{m}{n+1}$] and (b) position [$p_m = \frac{m-0.3}{n+0.4}$].

The time for a random event generator can be derived (Bury, 1999) using

$$t = -10^{-a} \ln(v), \tag{13}$$

where t is a random time interval between events and v is a random number at the interval (0,1).

Therefore, the probability of at least one earthquake of magnitude $\geq M$ within t years is

$$p = 1 - e^{-Nt} = 1 - e^{-(10^{a-bM})*t}. \tag{14}$$

On this basis, we use equations (12–14) to simulate the magnitudes, probabilities, and time of future earthquakes. Figure 3 shows one example of random simulations so that each value of magnitude and probability for each time interval is not a fixed value. This figure also indicates the probability of the same magnitude increases with time and that the probability of low magnitude is higher than the probability of high magnitude for each time interval.

Data Processing and Results

First, we divide Taiwan into 391 grids at a grid interval of 0.1° latitude by 0.1° longitude. From Figure 1, we can see that earthquake data are ample. We select earthquakes of magnitude $M_w \geq 5.0$ and focal depths ≤ 35.0 km using the same complete earthquake dataset as Chen *et al.* (2010). By applying the attenuation laws for PGA and peak ground velocity (PGV), we are able to determine maximum PGA and maximum PGV for each grid. We further combine the PGA

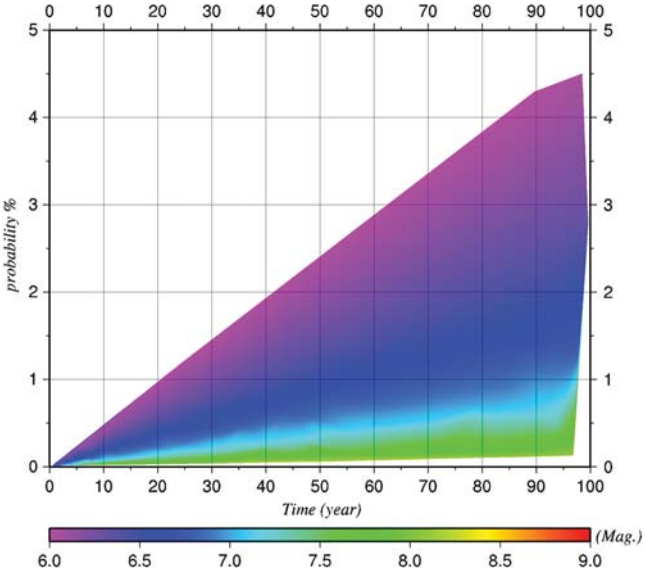

Figure 3. An example to show that probability, magnitude, and time are not fixed values of random simulating of future earthquakes with magnitude $M_w \geq 6.0$ for Taiwan; that the probability of the same magnitude increases with time; and that the probability of low magnitude is higher than the probability of high magnitude for each time interval.

and PGV values to obtain corresponding modified Mercalli intensity (MMI) values (Wald *et al.*, 1999) (Fig. 4). The MMI is the intensity scale used in the United States of America. This scale is based on 12 levels, from unfelt shaking to catastrophic destruction, and on observed effects rather than a mathematical basis. From Figure 4, we can see maximum PGA, maximum PGV, and maximum MMI follow a path extending from Hsinchu southward to Taichung, Chiayi, and Tainan in western Taiwan, and a path from Ilan southward to Hualian and Taitung in eastern Taiwan. To obtain the a- and b-values for each grid we use $\log_{10}(N) = a - b\log_{10}(\text{PGA})$, $\log_{10}(N) = a - b\log_{10}(\text{PGV})$, and $\log_{10}(N) = a - bI$. The regions with high PGA and PGV values are often associated with low b-values (Fig. 5). It indicates future earthquakes can be expected along zones characterized by low b-values. This pattern suggests that these areas can expect future strong shaking (Wyss and Stefansson, 2006).

To verify these findings for low b-values, and increase the data volume and therefore the confidence level returned from each grid, we divide Taiwan into grids of 0.2° latitude by 0.2° longitude, then apply the Gumbel (1958) probability plot for a- and b-values of each grid and match equations (12–14) to simulate the probabilities of future earthquakes of $M_w \geq 6.0$ for the next 10, 20, 30, and 50 years (Fig. 6). From Figure 6, once again the higher probability paths for large earthquakes are from Hsinchu southward to Taichung, Chiayi, Tainan, and Kaohsiung in western Taiwan, and from Ilan southward to Hualian and Taitung in eastern Taiwan.

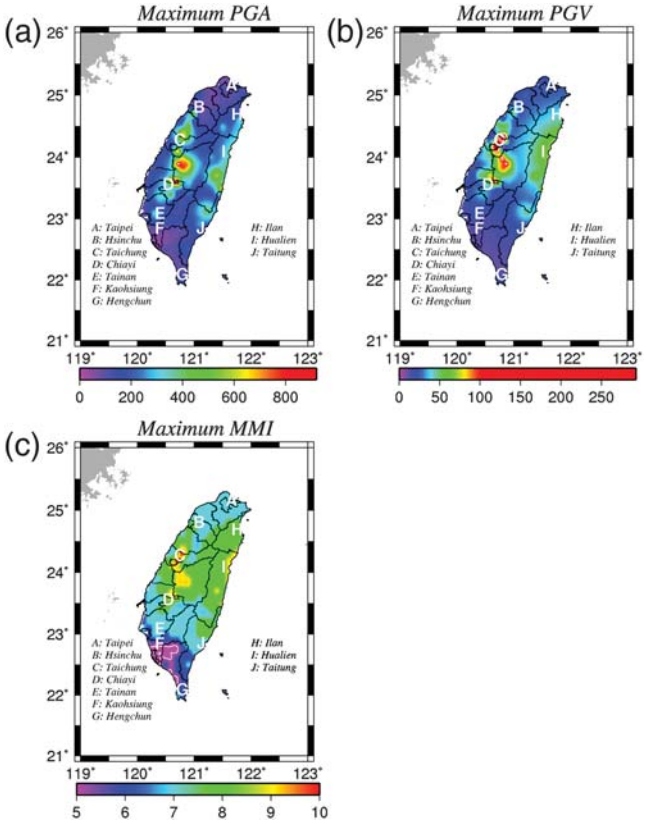

Figure 4. The contour of maximum PGA, maximum PGV, and maximum MMI of each grid. Maximum PGA, PGV, and MMI are along a zone extending from Hsinchu southward to Taichung, Chiayi, and Tainan in western Taiwan, and a zone extending from Ilan southward to Hualian and Taitung in eastern Taiwan.

Conclusion

In this study, we use the augmented, homogenized (in terms of moment magnitude), historic earthquake catalog for Taiwan to determine a- and b-values for eastern and western Taiwan as well as PGA, PGV, and MMI for both regions. The results are then verified using extreme value theory. Taiwan is gridded at a grid size of 0.1° latitude by 0.1° longitude. The attenuation laws for PGA and PGV are applied for each grid,

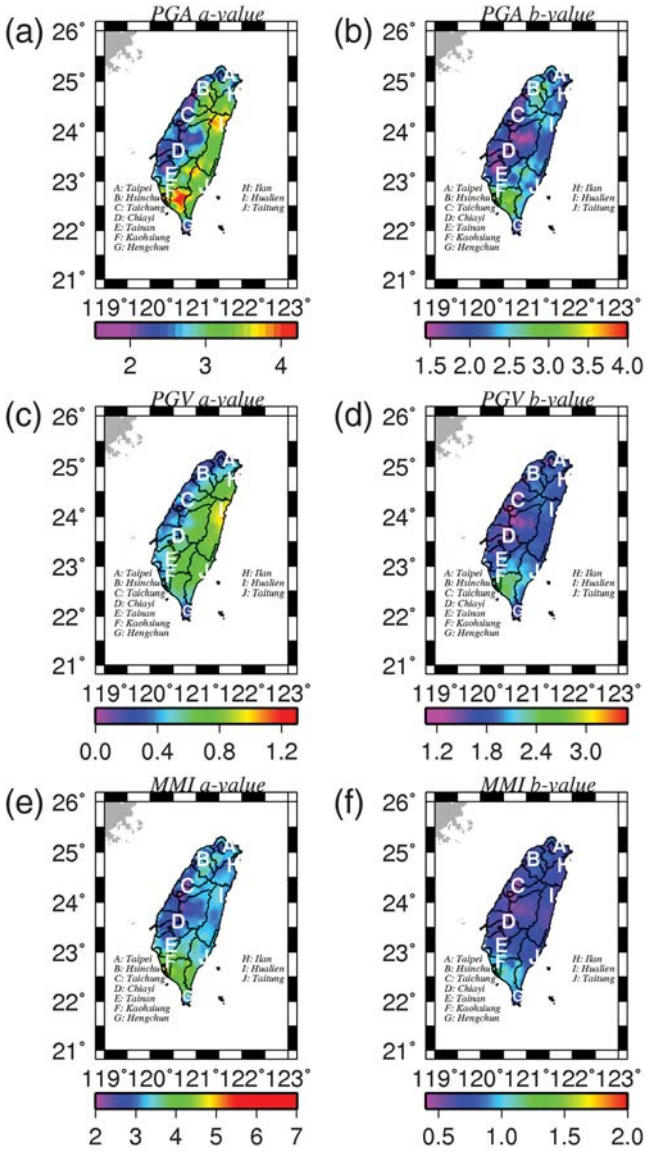

Figure 5. The contour of a- and b-values of $\log_{10}(N) = a - b\log_{10}(\text{PGA})$, $\log_{10}(N) = a - b\log_{10}(\text{PGV})$, and $\log_{10}(N) = a - bI$ of each grid. The path of low b-values is the same as maximum PGA, maximum PGV, and maximum MMI.

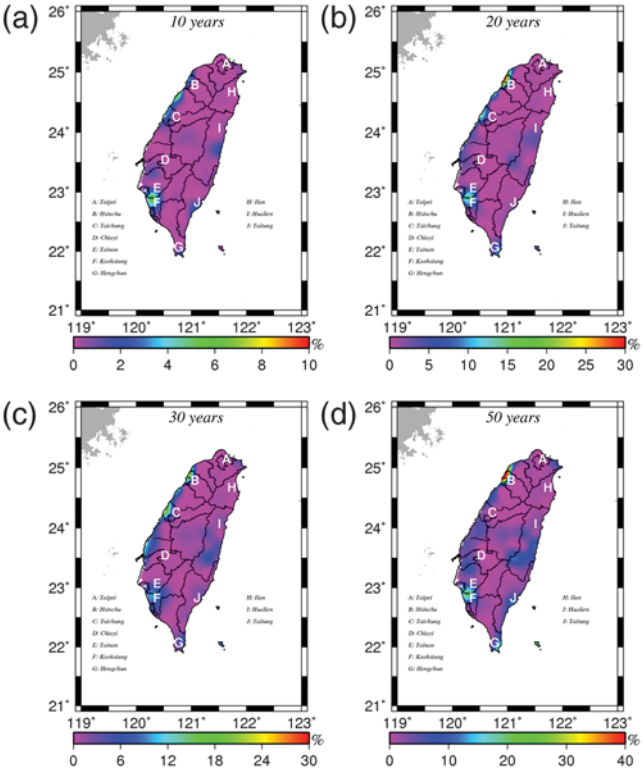

Figure 6. Simulating the probability that earthquakes with $M_w \geq 6.0$ will occur within the next (a) 10 years, (b) 20 years, (c) 30 years, and (d) 50 years. The higher probabilistic path is similar to the low $M_w \geq 6.0$ values trend.

and PGA and PGV determined. The combined PGA and PGV are used to estimate MMI at each grid The *a*- and *b*-values are also determined for the 0.1° by 0.1° grids. Finally, *b*-values are verified using extreme value theory, and Gumbel equations are applied to Taiwan for a grid size of 0.2° latitude by 0.2° longitude. The larger grid size increases the confidence level of the results obtained for *b*-values. The results of both analyses show that maximum PGA, maximum PGV, and maximum MMI follow a path extending from Hsinchu southward to Taichung, Chiayi, and Tainan in western Taiwan, and a path from Ilan southward to Hualian and Taitung in eastern Taiwan. The determination of *b*-values for Taiwan shows that these paths also correspond to paths of low *b*-values, indicating that future earthquakes can be expected along zones characterized by low *b*-values.

Data and Resources

All data sources are taken from published works listed in the References. Some plots were made using Generic Mapping Tools, version 4.3.1 (www.soest.hawaii.edu/gmt, last accessed August 2006; Wessel and Smith, 1998).

Acknowledgments

This study was supported by NSC 99-2116-M-570-001.

References

Bury, K. (1999) *Statistical Distributions in Engineering*, Cambridge University Press, Cambridge, ISBN 0-521-63506-3.

Chen, K. P., and Y. B. Tsai (2008). A catalog of Taiwan earthquakes (1900–2006) with homogenized M_w magnitudes, *Bull. Seismol. Soc. Am.* **98,** 483–489.

Chen, K. P., Y. B. Tsai, C. T. Cheng, K. S. Liu, and W. Y. Chang (2010). Estimated seismic intensity distributions for earthquakes in Taiwan from 1900 to 2008, *Bull. Seismol. Soc. Am.* **100,** 2905–2913, doi: 10.1785/0120090397.

Fisher, R. A., and L. H. C. Tippett (1928). Limiting forms of the frequency distribution of the largest or smallest member of a sample, *Proc. Cambridge Phil. Soc.* **24,** no. 180.

Gumbel, E. J. (1958), *Statistics of Extremes*, Dover Publications Edition 2004, originally published Colombia University Press, ISBN 0 486 43604 7.

Gutenberg, B., and F. Richter (1944). Frequency of earthquakes in California, *Bull. Seismol. Soc. Am.* **34,** 185–188.

Johnson, N. L., S. Kotz, and N. Balakrishnan (1995), *Continuous Univariate Distributions*, Second Ed., Vol. **2**, John Wiley and Sons, New York, ISBN 0-471-58494 0.

Lomnitz, C. (1974). Global tectonics and earthquake risk, in *Developments in Geotectonics*, Vol. **5**, Elsevier Scientific Publishing Company, New York.

Turnbull, M., and D. Weatherley (2006). Validation of using Gumbel probability plotting to estimate Gutenberg-Richter seismicity parameters, 24–26 November, Earthquake Engineering Australia, Canberra, 127–135.

Wald, D. J., V. Quitoriano, T. H. Heaton, H. Kanamori, C. W. Scrivner, and C. B. Worden (1999). Trinet "ShakeMaps": Rapid generation of peak ground motion and intensity maps for earthquakes in southern California, *Earthq. Spectra* **15,** 537–555.

Wessel, P., and W. H. F. Smith (1998). New, improved version of Generic Mapping Tools released, *Eos Trans. AGU* **79,** 579.

Wyss, M., and R. Stefansson (2006), Nucleation points of recent mainshocks in southern Iceland, mapped by *b*-values, *Bull. Seismol. Soc. Am.* **96,** 599–608.

Hsin Sheng College of Medical Care and Management
No. 418, Gaoping Sec., Jhongfong Rd.
Longtan, Taoyuan County 32544
Taiwan
chenkueipao@yahoo.com.tw
(K.-P.C.)

Geosciences Department, Pacific Gas and Electric Company
One Market, Spear Tower
Suite 2400 San Francisco
CA 94105-1126
(Y.-B.T.)

Department of Natural Resources and Environmental Studies
National Dong Hwa University
No. 1, Sec. 2, Da Hsueh Rd.
Shoufeng, Hualien 97401
Taiwan
(W.-Y.C.)

Sinotech Engineering Consultants. Inc.
No. 171, Nanking E. Rd.
Sec. 5, Taipei 105
Taiwan
(C.-T.C.)

Manuscript received 4 September 2011